

Small variations in multiple parameters account for wide variations in HIV-1 set-points: a novel modelling approach

Viktor Müller^{1†}, Athanasius F. M. Marée² and Rob J. De Boer^{2*}

¹Department of Plant Taxonomy and Ecology, Eötvös Loránd University, Budapest, Hungary

²Department of Theoretical Biology, Utrecht University, Padualaan 8, 3584 CH Utrecht, The Netherlands

Steady-state levels of HIV-1 viraemia in the plasma vary more than a 1000-fold between HIV-positive patients and are thought to be influenced by several different host and viral factors such as host target cell availability, host anti-HIV immune response and the virulence of the virus. Previous mathematical models have taken the form of classical ecological food-chain models and are unable to account for this multifactorial nature of the disease. These models suggest that the steady-state viral load (i.e. the set-point) is determined by immune response parameters only. We have devised a generalized consensus model in which the conventional parameters are replaced by so-called 'process functions'. This very general approach yields results that are insensitive to the precise form of the mathematical model. Here we applied the approach to HIV-1 infections by estimating the steady-state values of several process functions from published patient data. Importantly, these estimates are generic because they are independent of the precise form of the underlying processes. We recorded the variation in the estimated steady-state values of the process functions in a group of HIV-1 patients. We developed a novel model by providing explicit expressions for the process functions having the highest patient-to-patient variation in their estimated values. Small variations from patient to patient for several parameters of the new model collectively accounted for the large variations observed in the steady-state viral burden. The novel model remains in full agreement with previous models and data.

Keywords: HIV; modelling; parameter variations; food-chain model; viral load

1. INTRODUCTION

HIV-1 infection is characterized by high levels of virus in both the plasma and lymph nodes of infected individuals during all stages of the disease (Embretson *et al.* 1993; Pantaleo *et al.* 1993; Piatak *et al.* 1993). After an initial peak of viraemia in primary infection, virus levels stabilize around a certain set-point and typically increase only slowly thereafter (Weiss 1993; Mellors *et al.* 1996). The viral load is a steady-state balance between ongoing extensive virus replication and rapid clearance (Ho *et al.* 1995; Wei *et al.* 1995; Perelson *et al.* 1996). The level of this steady state, as reflected by the virus titre in peripheral blood, shows enormous variation from patient to patient. Even after discarding the highest measurements, the variation remains over 1000-fold (Piatak *et al.* 1993). Moreover, the set-point is strongly correlated with the rate of progression (Mellors *et al.* 1996). The steady-state viral burden is influenced by several different host and viral factors including target cell availability (De Boer & Perelson 1998; De Boer *et al.* 1998; Orendi *et al.* 1998), the humoral immune response (Fauci 1993), the cellular immune response (Borrow *et al.* 1994; Rinaldo *et al.* 1995; Borrow *et al.* 1997; Goulder *et al.* 1997; Ogg *et al.* 1998; Jin *et al.* 1999; Schmitz *et al.* 1999) and virulence factors (Deacon *et al.* 1995; Katzenstein *et al.* 1996).

Mathematical models of HIV-1 infection typically have the form of an ecological food-chain model, with target

cells as the prey, productively infected cells as their predator and the immune response as the top predator (Nowak & Bangham 1996; De Boer & Perelson 1998). A major problem with such models in both ecology (Arditi & Ginzburg 1989; Ginzburg & Akçakaya 1992; Abrams 1994; Kaunzinger & Morin 1998) and virology (De Boer & Perelson 1998) is the strong dependence of steady-state results on the precise form and length of the food chain. For instance, in a typical cytotoxic T-cell model, large variations in the HIV-1 burden require a similar variation in a parameter called the 'immune responsiveness' (Nowak & Bangham 1996). However, such a variation, which spans several orders of magnitude, is not easily accounted for by a single biological attribute. Rather, it is expected that several factors contribute to the variation. Indeed, the experimental evidence cited above suggests that several factors besides immune responsiveness play a role.

Complications like this are typical of mathematical food-chain models. A famous example from ecology is the 'paradox of enrichment' (Rosenzweig 1971), where increasing the food availability of a prey population fails to increase the steady-state level of that population. Rather, it is the next level of the food chain, i.e. the predator, that profits from the enrichment by an increase in its steady-state level. Conversely, in a three-dimensional food chain consisting of a prey, a predator and a top predator population, only the prey and the top predator ultimately benefit from an enrichment of the food availability of the prey. Generally, the correlations between the steady states of the different populations in food-chain models are determined by (i) the number of populations

* Author for correspondence (r.j.deboer@bio.uu.nl).

† Present address: Collegium Budapest, Institute for Advanced Study, Szentháromság u.2., H-1014 Budapest, Hungary.

in the food chain, (ii) saturation effects within the different populations, and (iii) competition effects within the different populations (Arditi & Ginzburg 1989; Ginzburg & Akçakaya 1992; Abrams 1994; Kaunzinger & Morin 1998). Whether or not mathematical models are in agreement with, for example, the observed negative correlation between the specific CD8⁺ T-cell immune response and the viral load (Ogg *et al.* 1998) or with the positive correlation between the viral load and target cell levels (Orendi *et al.* 1998) does not rest on a generic property of the models. Instead, it depends on the length of the food chain of the model and/or on the precise form of the interaction terms.

Developing mathematical models for HIV-1 infection that are simple enough to allow a good understanding and realistic enough to allow small variations in several factors to account collectively for large variations in the viral burden during the asymptomatic quasi-steady state remains a major challenge. The main objective of this paper is to pick up this challenge by developing a novel heuristic approach that allows the identification of the processes controlling the steady-state levels. The approach is applied here to a discussion of the factors controlling HIV-1 during clinical latency.

2. A CONSENSUS MODEL WITH 'PROCESS FUNCTIONS'

We adopt a widely used minimal model of an HIV-1 infection (Nowak & Bangham 1996; Bonhoeffer *et al.* 1997*a,b*; De Boer & Perelson 1998) written in the 'Arden notation' (<http://www-binf.bio.uu.nl/~rdb/arden.html>). The model considers target cells T , productively infected cells I , virus V and immune effector CD8⁺ T cells E . The structure of the model resembles an ecological food chain of a prey T , its predator I with a life stage V and a top predator E (De Boer & Perelson 1998). Since the steady-state levels during HIV-1 clinical latency are changing on a very slow time-scale of years, one typically studies the equilibria of the model. The novelty of our approach resides in the interpretation of the parameters of the model: any 'parameter' in equations (1)–(4) is explicitly allowed to be any function of the other 'parameters' and/or variables of the model. Because each 'parameter' in fact reflects a process, we call each of them a 'process function'. For example, the process σ by which target cells are produced could be written as $\sigma = aQ$, where aQ represents the activation a of quiescent cells Q (Stilianakis *et al.* 1997); the process α of the activation of the immune response could be written as a saturation function $\alpha = a/(h + I)$ (De Boer & Perelson 1998) and the death process δ of infected cells could be made dependent on the immune response $\delta = kE$, where k is the killing rate. This interpretation of parameters as processes allows us to postpone the specification of the interaction between the immune response E and equations (1)–(4). Thus, we first obtain generic results that are truly independent of the form of this interaction.

We write our generalized consensus model as follows:

$$\frac{dT}{dt} = \sigma - \delta_T T - \beta TV, \quad (1)$$

$$\frac{dI}{dt} = f\beta TV - \delta I, \quad (2)$$

$$\frac{dV}{dt} = pI - cV, \quad (3)$$

$$\frac{dE}{dt} = \alpha EI - \delta_E E, \quad (4)$$

where the process function σ is the source of target cells, β is an infection process, f is the fraction of successful infections, p represents the rate of virion production, c is the virion clearance rate and α is the immune responsiveness. All process functions δ determine death rates. One can easily see that this comprises a three-dimensional food chain because the fast time-scale of equation (3) typically allows for its replacement by the quasi-steady-state assumption $V = (p/c)I$.

One obtains the steady-state expressions

$$\hat{I} = \frac{\delta_E}{\alpha}, \quad (5)$$

$$\hat{V} = \frac{p}{c} \hat{I}, \quad (6)$$

and

$$\hat{T} = \frac{\sigma}{\delta_T + \beta \hat{V}} = \frac{c\alpha\sigma}{c\alpha\delta_T + p\beta\delta_E} \quad (7)$$

from equations (4), (3) and (1), respectively. Equation (5) suggests that the only factors determining the steady-state level of productively infected cells \hat{I} are the 'immune responsiveness' α and the death rate of immune effectors δ_E (Nowak & Bangham 1996). Because one expects δ_E to vary little between patients, large variations in \hat{I} would require similar variations in α . Other factors such as target cell availability and viral virulence seem to have no effect whatsoever in controlling \hat{I} because they are not reflected in either δ_E or α . This is a generalization of an earlier study (Nowak & Bangham 1996) because we have not specified the effect of the immune response on the system beforehand.

Formally, it is not known whether patients differing by orders of magnitude in their viral load in the peripheral blood (Mellors *et al.* 1996) also have large differences in the total body counts of productively infected cells \hat{I} . From equation (6), differences in the viral production p and in the viral clearance c could contribute to the observed variations in \hat{V} . However, there is little indication that patients differ markedly in p (Haase *et al.* 1996; Hockett *et al.* 1999) or in c (Perelson *et al.* 1996; Mittler *et al.* 1999; Ramratnam *et al.* 1999). Moreover, there is good correlation between the numbers of productively infected cells and the amounts of virus in the lymphoid tissue or in the peripheral blood (Hockett *et al.* 1999). Finally, the fact that the viral burden in the peripheral blood is a good predictor of the rate of disease progression (Mellors *et al.* 1996) also suggests that patients with a high viral load do have a severe infection, i.e. do have a high \hat{I} . In this paper we therefore wish to explain large differences in \hat{I} with small differences in parameter values. Equation (5) fails to account for this: large differences in \hat{I} require large differences in α .

Because there is no explicit connection between equation (4) and the rest of the system, we cannot

determine the steady state \hat{E} . However, for the special case where $\hat{E} = 0$ or where \hat{E} is at a constant (e.g. maximum) level, one can drop equation (4) from the system and obtain a target-cell-limited solution (McLean *et al.* 1991; McLean & Nowak 1992; De Boer & Perelson 1998) from equations (2), (1) and (3), respectively, i.e.

$$\hat{T} = \frac{\delta c}{f\beta p}, \quad (8)$$

$$\hat{I} = \frac{\sigma f}{\delta} - \frac{\delta_T c}{\beta p}, \quad (9)$$

and

$$\hat{V} = \frac{p}{c} \hat{I}. \quad (10)$$

These steady-state expressions differ radically from the expressions in equations (5)–(7). This illustrates the problem outlined in §1, i.e. that steady states in a food-chain model depend crucially on its form and length (Arditi & Ginzburg 1989; Ginzburg & Akçakaya 1992; Abrams 1994; Kaunzinger & Morin 1998).

3. PUBLISHED ESTIMATED VALUES

Several steady-state values of the process functions and the variables of this consensus model have been estimated previously. For the turnover of productively infected cells we use the consensus estimate of $\delta \simeq 0.5/d$ (Ho *et al.* 1995; Wei *et al.* 1995; Klenerman *et al.* 1996; Perelson *et al.* 1996; Notermans *et al.* 1998). Between patients there is remarkably little variation in δ . Recent plasmapheresis experiments have provided novel estimates of 40–110 min for the half-life of HIV virions (Mittler *et al.* 1999; Ramratnam *et al.* 1999). An intermediate value is therefore 75 min, i.e. $c = 13/d$, but little is known about the patient-to-patient variation in c . Estimates for the production rate p vary between a few hundred (Haase *et al.* 1996) and a few thousand (Hockett *et al.* 1999). The latter study suggested that there is little variation in p between patients differing markedly in their viral burden (Hockett *et al.* 1999). The death rate of HIV-1-specific CD8⁺ effector cells during anti-retroviral therapy has been estimated by a tetramer assay as $\delta_E = 0.015/d$ (Ogg *et al.* 1999). Most of the virus is trapped on the surface of follicular dendritic cells (FDCs) (Pantaleo *et al.* 1993; Hockett *et al.* 1999), with an average pool size of order of magnitude 10^{10} particles in the lymphoid tissue (Cavert *et al.* 1997). In different studies addressing the lymphoid tissue, the total body counts of productively infected cells have varied between 10^7 (Chun *et al.* 1997) and 10^8 (Cavert *et al.* 1997).

We will assume here that dividing CD4⁺ T cells form the main pool of target cells. Since, for human CD4⁺ T cells, cell division takes approximately a day (Fleury *et al.* 1998), we assume that $\delta_T \simeq 1/d$. Identifying dividing CD4⁺ T cells in the lymphoid tissue with the Ki67 monoclonal antibody yields estimates varying around 10^9 target cells (Fleury *et al.* 1998; Zhang *et al.* 1998). In addition, labelling studies with ²H-glucose have suggested that the percentage of dividing CD4⁺ T cells is 1% in healthy controls and 3–5% in HIV-1 patients (Hellerstein *et al.* 1999). Having approximately 2.5×10^{11} CD4⁺

T cells this also suggests a total body count of approximately 10^9 target cells.

(a) Estimating values of process functions

The approach developed here is an attempt to breach the non-robustness of results obtained by solving for steady-state levels in food-chain models. In order to obtain generic results a ‘consensus’ model that is a generalization of many different more detailed models having different explicit expressions for the different process functions is required. The model in equations (1)–(4) is a good example of such a consensus model. Here we solve the inverse problem of estimating the values of process functions by substitution of observable parameters and steady states into equations (1)–(4). Because the values of the process functions are solved directly from the steady state of the differential equations, these values remain valid for all possible functional realizations of the consensus model. Thus, any such estimate provides a generic numerical value of the corresponding process for the particular steady state at hand. Process functions with little variation in their estimated values can be explicitly written as constants, i.e. as parameters. On the other hand, finding a large patient-to-patient variation in the estimated values of a process function suggests an explicit expression involving variables and novel parameters.

Thus, we estimate the values of process functions in terms of observable steady-state levels \hat{T} , \hat{I} and \hat{V} and measured parameter values δ and δ_E . Rewriting equation (3) yields an estimate for the production scaled by the clearance time, i.e.

$$p/c = \hat{V}/\hat{I}, \quad (11)$$

and rewriting equation (4) gives

$$\alpha = \delta_E/\hat{I}. \quad (12)$$

The steady state of equation (2) gives

$$\beta = \frac{\delta}{f} \frac{\hat{I}}{\hat{V}\hat{T}} = \frac{\delta c}{f\hat{p}\hat{T}}, \quad (13)$$

and, hence, from equation (1) we obtain that

$$\sigma = \delta_T \hat{T} + \frac{\delta}{f} \hat{I}. \quad (14)$$

Note again that these expressions are obtained for any form of immune control in the consensus model, i.e. they are obtained without specifying the interaction between the immune effectors E and the remainder of the system.

In order to illustrate basic principles, we estimate the values of process functions from previously published data on approximately ten HIV-1-infected asymptomatic patients. The data in table 1 compile estimates from three different papers providing (i) \hat{I} and \hat{V} , i.e. the number of productively infected cells and virions trapped on FDCs in lymphoid tissue (Cavert *et al.* 1997), (ii) \hat{T} , i.e. the number of dividing CD4⁺ T cells in lymphoid tissue (Zhang *et al.* 1998), and (iii) δ , i.e. the death rates of productively infected cells (Notermans *et al.* 1998). Knowing \hat{I} and \hat{V} we can estimate p/c from equation (11). Since there is no information on the value of f , we calculate $f\beta$ from equation (13). Not knowing f we are not yet

Table 1. Clinical data and the corresponding numerical estimates

(The number of productively infected cells \hat{I} was calculated from table 1 in Cavert *et al.* (1997) by multiplying the column ‘number of mononuclear cells (MNC) per gram of lymphoid tissue (LT) with >20 copies of HIV per cell’ by the expected 700 g of lymphoid tissue in a 70 kg individual. Similarly, the steady-state viral burden \hat{V} in lymphoid tissue was calculated by multiplying the column ‘number of copies of HIV RNA per gram of LT on follicular dendritic cells (FDC)’ in the same table by 0.5×700 because viral RNA is double stranded and because of the 700 g of lymphoid tissue. Because the vast majority of the virions are associated with FDCs in lymphoid tissue (Cavert *et al.* 1997), this should provide a fair estimate of the total body burden. The number of target cells \hat{T} was calculated from table 2 in Zhang *et al.* (1998) by multiplying the CD4⁺ T cell count per microgram of lymphoid tissue by 700×10^6 and by the fraction of Ki67⁺ CD4⁺ in lymphoid tissue. The death rates δ of productively infected cells were copied from table 1 in Notermans *et al.* (1998). The values are estimated by the expressions in equations (11)–(14) derived in the text. Constant parameter values: $\delta_T = 1$, $\delta_I = 0.1$, $\delta_E = 0.015$, $E_0 = 8$, $k = 10$, $a = 1$ and $h = 10^6$. The identification number of each patient in column 1 is a compilation of those used in Cavert *et al.* (1997), Notermans *et al.* (1998) and Zhang *et al.* (1998), respectively.)

ID number	\hat{I} (cells)	\hat{V} (virions)	\hat{T} (cells)	δ (day ⁻¹)	α (cell ⁻¹ day ⁻¹)	p/c virions cell ⁻¹)	$f\beta$ (virions ⁻¹ day ⁻¹)	ε (% ⁻¹)	β (virions ⁻¹ day ⁻¹)	σ (cells day ⁻¹)	\hat{E} (%)	f
typical	10 ⁸	10 ¹⁰	10 ⁹	0.50	1.5 × 10 ⁻¹⁰	100	5 × 10 ⁻¹²	40.6	8.5 × 10 ⁻¹¹	1.9 × 10 ⁹	1.60	0.059
48 910	3.2 × 10 ⁸	10 ¹¹	—	0.37	4.7 × 10 ⁻¹¹	326	—	54.8	—	—	1.19	0.077
49 021	6.8 × 10 ⁸	5.6 × 10 ¹⁰	1.1 × 10 ⁹	0.89	2.2 × 10 ⁻¹¹	82	10 ⁻¹¹	70.2	1.1 × 10 ⁻¹⁰	7.3 × 10 ⁹	0.93	0.097
44 935	1.8 × 10 ⁸	1.2 × 10 ¹¹	1.4 × 10 ⁹	0.34	8.6 × 10 ⁻¹¹	700	3.4 × 10 ⁻¹³	46.4	5.1 × 10 ⁻¹²	2.3 × 10 ⁹	1.41	0.066
45 242	2.8 × 10 ⁷	7 × 10 ⁹	1.3 × 10 ⁹	0.51	5.4 × 10 ⁻¹⁰	250	1.5 × 10 ⁻¹²	31.0	3.3 × 10 ⁻¹¹	1.6 × 10 ⁹	2.04	0.047
49 156	3.5 × 10 ⁸	7 × 10 ¹⁰	1.4 × 10 ⁹	0.46	4.3 × 10 ⁻¹¹	200	1.6 × 10 ⁻¹²	56.2	2 × 10 ⁻¹¹	3.5 × 10 ⁹	1.16	0.079
49 777	9.8 × 10 ⁷	4.6 × 10 ¹⁰	3.1 × 10 ⁸	0.60	1.5 × 10 ⁻¹⁰	464	4.1 × 10 ⁻¹²	40.4	7 × 10 ⁻¹¹	1.3 × 10 ⁹	1.61	0.059
49 684	1.4 × 10 ⁸	2.2 × 10 ¹⁰	5.1 × 10 ⁸	0.37	1.1 × 10 ⁻¹⁰	155	4.6 × 10 ⁻¹²	43.9	7.3 × 10 ⁻¹¹	1.3 × 10 ⁹	1.48	0.063
44 699	4.6 × 10 ⁷	8.8 × 10 ⁹	—	0.52	3.3 × 10 ⁻¹⁰	192	—	34.3	—	—	1.87	0.051
48 503	10 ⁸	4.6 × 10 ¹⁰	1.5 × 10 ⁹	0.36	1.4 × 10 ⁻¹⁰	433	5.6 × 10 ⁻¹³	41.1	9.4 × 10 ⁻¹²	2.1 × 10 ⁹	1.58	0.059
ratio	24	17	4.8	2.4	24	8.5	29	2.3	22	5.6	2.2	2.1

able to use equation (14) in estimating σ . As noted above, the estimates listed in table 1 reflect true ‘values’ of the corresponding process in that patient. The variation in these estimates therefore provides generic information about the variation in the processes determining the viral load in each patient. As a measure of the variation in each column, the bottom row of table 1 shows the ratio of the highest over the lowest value of each variable or process. The first line of table 1 gives a ‘typical patient’, corresponding to a rounded average of the data.

The variation in this data set seems considerably less than the typical orders of magnitude variation (Mellors *et al.* 1996). The variations in \hat{V} and \hat{I} are ‘only’ 17-fold and 24-fold, respectively (see table 1). This is partly due to the fact that we considered the lymphoid tissue. In peripheral blood the variation in the viral load is approximately 100-fold (Notermans *et al.* 1998). However, in this patient set, the viral load in the peripheral blood is not correlated with either \hat{V} or \hat{I} in the lymphoid tissue. Because the total body viral load is largely confined to the lymphoid tissue, here we only consider lymphoid tissue data. We will return to the issue of explaining the orders of magnitude variation in figure 1.

Although we found a reasonable correlation between \hat{I} and \hat{V} ($r = 0.79$ and $p < 0.01$) in this study, the 8.5-fold variation in p/c demonstrates that there is still considerable variation in the \hat{V}/\hat{I} ratio. Note that there is a discrepancy with the study of Hockett *et al.* (1999) who found \hat{V}/\hat{I} ratios that were an order of magnitude larger. This is probably due to different measurement techniques. In the data sets used for the present paper and with the intermediate estimate of $c = 13/d$ (Mittler *et al.* 1999; Ramratnam *et al.* 1999) we obtained production rates p of

a few thousand virions per cell per day. The observed 8.5-fold variation could obviously be due to patient differences in c , p or in the retention of virus particles in the lymphoid tissue. Finally, the two process functions that vary most are α and $f\beta$.

4. EXPLICIT EXPRESSIONS FOR PROCESS FUNCTIONS

(a) The cytotoxic model

One can retrieve previous cytotoxic control models by allowing the process δ to depend on the immune response. For example, one could write

$$\delta = \delta_I + \alpha kE,$$
 (15)

or

$$\delta = \delta_I + kE,$$
 (16)

where δ_I is the normal death rate and kE represents the cytotoxic killing of productively infected cells. In the model of Nowak & Bangham (1996) the killing is weighted by the immune responsiveness α , as in equation (15). Using equations (11)–(14) and setting $f = 1$, one can again calculate α , p/c , β and σ for every patient in table 1 in order to obtain the correct steady state with either of these models. The novel parameters δ_I and k only change the steady-state immune response \hat{E} and no other variable of the system. They can be changed freely provided that $\delta_I < \delta$ and $\hat{E} > 0$.

Having specified the effect of the immune response in equations (15) and (16) one may solve for the steady-state level \hat{E} . However, the form of the steady-state

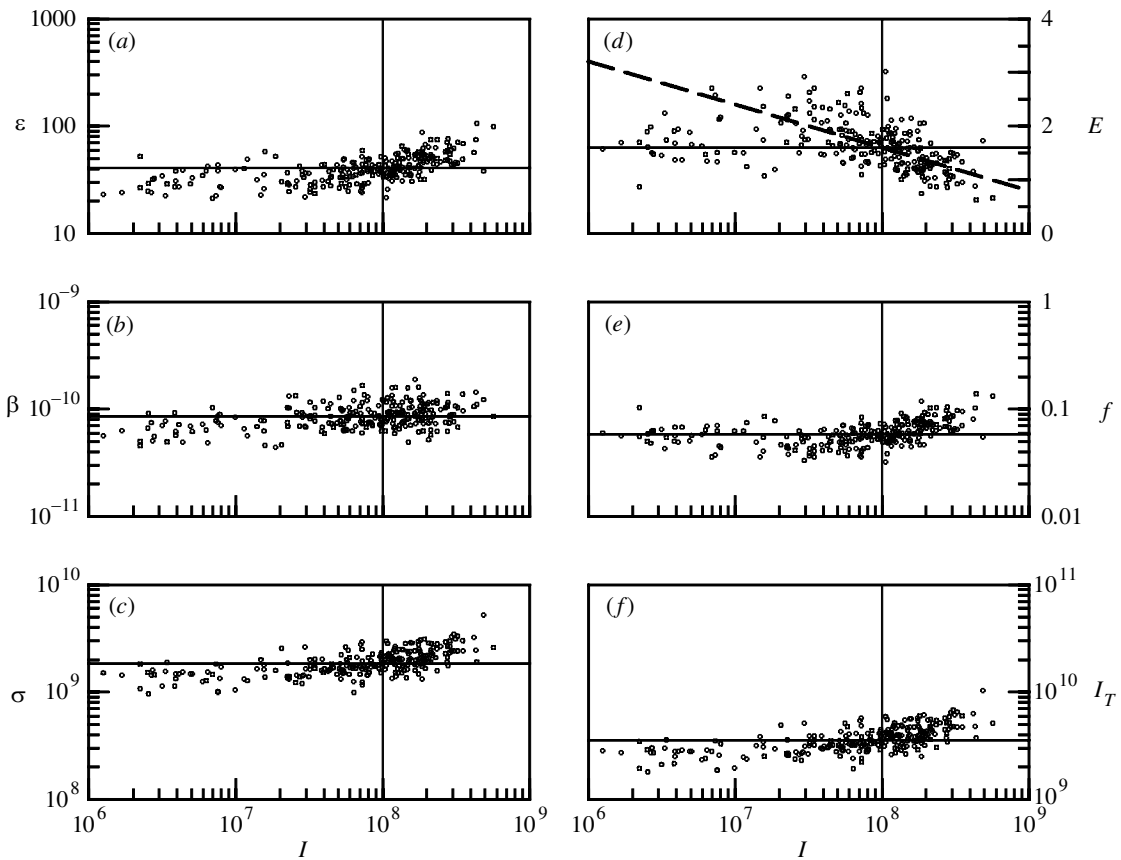


Figure 1. Analysis of the effects of small parameter variations in the 'early cytotoxic' model of equations (1)–(4), (17) and (18). The stable non-trivial equilibrium value I was calculated for 250 different parameter combinations of ε , β and σ and plotted against (a–c) the parameter values used, (d) the corresponding equilibrium value E , (e) the cytotoxicity level f , and (f) the potential 'target-cell-limited' level I_T in the case of an anti-CD8 treatment. The values of ε , β and σ were independently drawn from log-normal distributions, with a standard deviation such that 95% of the parameter values cover a threefold range around the estimated parameter values of the 'typical patient' (see table 1). All other parameters are as described in the legend to table 1. The parameter estimates and equilibrium values of the typical patient are indicated by the horizontal and vertical lines. (d) The dashed line indicates the Ogg *et al.* (1999) relationship. It is this figure that sets our estimate of E_0 : by setting $E_0 = 8$ in $\hat{E} = E_0 - 0.8 \log I$, we allow the rightmost patients (having $\hat{I} = 10^9$) to still have an immune response of $\hat{E} = 0.8\%$. At $\hat{I} = 10^{10}$ the immune response vanishes.

expression strongly depends on the form of the model. With equation (15) it is a non-monotonic function of the immune responsiveness α (Nowak & Bangham 1996) and with equation (16) it is an increasing saturation function of α . Moreover, one may study models that are totally independent of target cell levels by letting $f = 1/T$. In such models \hat{E} is either independent of α (with equation (16)) or an inverse function of α (with equation (15)). Thus, these four cytotoxic models all have different predictions for the relation between the steady-state immune response \hat{E} and α and, hence (see equations (5) and (6)), for the relation between \hat{E} and the viral load \hat{V} . Having such non-generic predictions it seems impossible to conclude whether or not cytotoxic control models are in agreement with the observed strong negative correlation between the viral burden \hat{V} and the cytotoxic immune response \hat{E} as reported by Ogg *et al.* (1998). Finally, in all of these models, the large variation in the viral burden can only be attributed to large variations in the immune responsiveness α (and, more unlikely, in the turnover of the immune response δ_E) (see equation (5) and Nowak & Bangham (1996)). We have argued above that such large variations in α are likely to involve a number of hidden factors.

(b) Employing the variation in the estimated values

An important point of this paper is using the differences in the patient-to-patient variation in the various process functions in order to incorporate more biology into the model. First, both α and $f\beta$ are process functions that vary widely. If the number of productively infected cells I generally varies by orders of magnitude between patients (Mellors *et al.* 1996), α would also have to vary by orders of magnitude (Nowak & Bangham 1996). To us this suggests that α is not a 'true' parameter and is, indeed, more likely to reflect a process. Second, there is generally little variation between HIV-1-positive patients in the turnover δ of productively infected cells (Ho *et al.* 1995; Wei *et al.* 1995; Klennerman *et al.* 1996; Perelson *et al.* 1996). By our process function approach this would suggest that δ can be explicitly expressed as a constant and that the cytotoxic expressions written above need not be the most appropriate choice for the effect of the immune response. An alternative possibility is that most of the infected cells are removed by cytotoxic T lymphocytes (CTLs) before they start to produce virus in large quantities (Klennerman *et al.* 1996). Since this can be incorporated by writing the process function f as an

explicit expression involving the immune response E , this would allow another process to account for part of the variation in $f\beta$. Because of the data supporting a role of target cell availability and viral virulence in setting the steady-state viral burden, \hat{I} should not only depend on the immune responsiveness α , but should also depend on the target cell production σ and the infection rate β . In the consensus model this is not the case because the form of equation (4) only allows for solving the steady state \hat{I} from the immune response equation. Replacing α by an expression allowing the proliferation of E to be a competitive saturation function of I (De Boer & Perelson 1998) allows one to tune parameters such that the steady state of equation (4) largely determines \hat{I} (i.e. for $\varepsilon \rightarrow 0$) or \hat{E} (i.e. for $h \rightarrow 0$).

These biological constraints can be implemented in the consensus model by writing the following expressions for our process functions:

$$\alpha = \frac{a}{h + I} \frac{1}{1 + \varepsilon E}, \quad (17)$$

and

$$f = \frac{1}{1 + kE}, \quad (18)$$

which allows for saturation in I and competition between the E cells, and the cytotoxic response eliminates a fraction of the recently infected cells. Note that δ now remains independent of E . Equations (17) and (18) represent an ‘early cytotoxicity’ functional realization of the consensus model of equations (1)–(4). The cytotoxic killing of infected cells predominantly takes place in the earlier stages of cellular infection before the infected cells start to produce virus in large quantities (Klennerman *et al.* 1996).

Setting proper values of the parameters of this model will yield the observed steady state. Thus, we can allow for more biology by imposing additional biological constraints on the values of ε , β and σ . The paper by Ogg *et al.* (1998) established a well-defined inverse relation between the steady-state viral load and the CD8⁺ T-cell response in the peripheral blood. From fig. 2B in Ogg *et al.* (1998) we read that $\log[\text{RNA}_{\text{plasma}}] \simeq \log[\text{RNA}_0] - 2\hat{E}$, where \hat{E} is the CTL response measured as the percentage of CTLs specific for HIV-1 epitopes. The paper by Hockett *et al.* (1999) allows us to compute the plasma RNA viral load from the number of productively infected cells in the tissue (i.e. I in the model) by their relationship $\log[\text{RNA}_{\text{plasma}}] \simeq \log[\text{RNA}_0] + 1.6 \log[\hat{I}]$. In combination, this yields the result that the expected immune response is $\hat{E} \simeq E_0 - 0.8 \log[\hat{I}]$. For our typical patient this gives $E \simeq 1.6\%$ as a typical value (see table 1). In addition, experiments with SIV-infected macaques where anti-CD8 treatment resulted in an enormous increase in the viral burden (Jin *et al.* 1999; Schmitz *et al.* 1999) have suggested that the CD8 immune response has a large impact on the steady-state viral burden. Setting $k = 10$ we achieve a removal of more than 95% of the infected cells (see the f -values in table 1). Thus, a rapid increase in the viral load is expected if one were to decrease E in order to simulate an anti-CD8 treatment (see below).

Having estimated \hat{E} from \hat{I} , we calculate the expected value of f from equation (18). Knowing the expected \hat{f} ,

we are able to compute β and σ from equations (13) and (14). Because we know that CD8⁺ effector T cells can proliferate relatively fast, i.e. $a \simeq 1 \text{ day}^{-1}$ and because we think that, due to the high antigen load, the immune response to HIV should typically be saturated, i.e. $h = 10^6 \ll \hat{I}$, we solve the competition parameter ε from equations (12) and (17) as

$$\varepsilon = \frac{1}{\hat{E}} \left(\frac{a\hat{I}}{\delta_E(h + \hat{I})} - 1 \right). \quad (19)$$

This procedure yields a complete estimation of all process functions for each individual patient in table 1. From the constraints imposed on the values of ε , β and σ , we naturally obtain steady states where the level of the immune response follows the ‘Ogg *et al.* (1998)’ relationship with the viral burden. In addition, the immune response very effectively clears recently infected cells in all patients, i.e. in all patients $f \ll 1$. The 24-fold variation in α is indeed resolved by small variations in ε and σ (see table 1). Equation (19) yields high values for ε , i.e. strong competition. CD8 immune responses could indeed be impaired during HIV infection due to a lack of HIV-specific helper T cells (Mori *et al.* 2000; Oxenius *et al.* 2000). Because $\varepsilon\hat{E} \gg 1$ and $h \ll \hat{I}$, the αEI proliferation term in equation (4) is approaching the ‘source’ term $\sigma_E = a/\varepsilon$. Apparently, we need only small variations in this source term.

The large variation in $f\beta$ has been resolved by small variations in f , but the variation in β has remained large. The reason for this is that, if patients have a high \hat{V}/\hat{I} ratio, then one obtains a high estimate for their scaled production rate p/c from equation (11). Hence, to account for their relatively low \hat{I} , a low estimate for β is obtained from equation (13). The large residual variation in β might be partly explained by different rates of retention in the lymphoid tissue, provided that free and bound virus particles have different infectivity.

The steady state turned out to be stable for all parameter values used in table 1 (and in figure 1). Although we have concentrated on a steady-state analysis, we did check how our ‘typical patient’ would respond to an anti-CD8 treatment (Jin *et al.* 1999; Schmitz *et al.* 1999) simulated by a large reduction of the effector population (e.g. $E = \hat{E}/100$). Decreasing E this much sharply increases f such that the viral load increases more than tenfold in a few days. The target cells decrease on a similarly rapid time-scale and a target-cell-limited steady state is monotonically approached. However, thanks to the high proliferation rate of $a = 1 \text{ day}^{-1}$, the effector population recovers on a time-scale of weeks. As a consequence, the viral load decreases and target cells recover and the pre-treatment equilibrium in table 1 is approached monotonically on a time-scale of weeks (not shown). This is in good agreement with other data (Jin *et al.* 1999; Schmitz *et al.* 1999).

In order to demonstrate that small parameter variations in this model can also account for the typically 1000-fold variations in the viral burden, we vary the values of ε , β and σ around their typical value in figure 1. Taking the typical value for each parameter from table 1 as the mean of a log-normal distribution we set the standard deviation such that 95% of the parameter

values cover at most a threefold range around the mean. Having drawn ε , β and σ independently, we compute the corresponding steady state of the system. We have plotted each actual parameter value with its corresponding steady state \hat{I} in figure 1a–c. Allowing for this threefold variation in ε , β and σ only, we obtain a variation of three orders of magnitude in \hat{I} . The immune response \hat{E} and cytotoxicity level f as they are realized by these parameter values are plotted in figure 1d,e. Figure 1f depicts the expected effect of the anti-CD8 treatment of Jin *et al.* (1999) and Schmitz *et al.* (1999). The steady-state viral burden expected in the absence of an immune response, i.e. \hat{I} as defined by equation (9), is plotted on the y-axis. Note that, over the entire range, this ‘target-cell-limited’ I_T level remains much higher than the ‘immune-controlled’ \hat{I} .

Our results demonstrate that, by the process function approach, we have indeed achieved what we aimed for. Variations in the viral burden are now collectively accounted for by variations in (i) the target cell production σ , (ii) the CD8 competition ε , and (iii) the infection rate β . Moreover, in order to account for the three orders of magnitude increase in the viral burden we only need a threefold variation in σ , β and ε . This seems a natural result because, by our present approach, processes varying widely are replaced by explicit expressions in terms of the dependent variables of the model and of new parameters. It thus becomes possible to account for the wide variation by combining smaller variations in several parameters and/or variables of the new model.

5. CONCLUSIONS

Obviously, our estimated values of the process functions remain crude approximations. For instance, it is probably not correct to assume that all Ki67⁺ CD4⁺ T cells are proper target cells for HIV-1. However, the estimates presented here mainly serve as an illustration of the process function approach that can be employed as a heuristic way of allowing experimental data to guide further model development. The parameter that retains most variation is the infection rate β . Indeed, β could be written as a function of the viral load V in order to reflect the differential trapping on the FDC network (Hockett *et al.* 1999).

Empirical studies into the factors controlling an HIV-1 infection during clinical latency have largely relied on correlating the steady-state viraemia with steady levels of the immune response (Ogg *et al.* 1998) and/or with target cell availability (Orendi *et al.* 1998). However, such an approach is not robust because different models predict radically different correlations. The inverse problem of estimating the values of processes from observed steady-state values gives far more robust results. In addition, the observed variations in these estimates suggested writing explicit expressions for the underlying process. This enabled us to develop novel models in which several factors collectively determine the steady-state viral burden in the asymptomatic phase.

We thank José Borghans and Lee Segel for helpful discussions. V.M. is supported by the Hungarian Scientific Research Fund (OTKA). A.F.M.M. is supported by the Priority Program

Nonlinear Systems of the Netherlands Organization for Scientific Research and R.J.D.B. is partially supported through the Theoretical Immunology Program of the Santa Fe Institute by the Jeanne P. and Joseph M. Sullivan Foundation. We thank Dr Daan Notermans for providing the combination of patient identifications required for producing table 1.

REFERENCES

- Abrams, P. A. 1994 The fallacies of ‘ratio-dependent’ predation. *Ecology* **75**, 1842–1850.
- Arditi, R. & Ginzburg, L. R. 1989 Coupling in predator–prey dynamics: ratio-dependence. *J. Theor. Biol.* **139**, 311–326.
- Bonhoeffer, S., Coffin, J. M. & Nowak, M. A. 1997a Human immunodeficiency virus drug therapy and virus load. *J. Virol.* **71**, 3275–3278.
- Bonhoeffer, S., May, R. M., Shaw, G. M. & Nowak, M. A. 1997b Virus dynamics and drug therapy. *Proc. Natl Acad. Sci. USA* **94**, 6971–6976.
- Borrow, P., Lewicki, H., Hahn, B. H., Shaw, G. M. & Oldstone, M. B. 1994 Virus-specific CD8⁺ cytotoxic T-lymphocyte activity associated with control of viremia in primary human immunodeficiency virus type 1 infection. *J. Virol.* **68**, 6103–6110.
- Borrow, P. (and 10 others) 1997 Antiviral pressure exerted by HIV-1-specific cytotoxic T lymphocytes (CTLs) during primary infection demonstrated by rapid selection of CTL escape virus. *Nature Med.* **3**, 205–211.
- Cavert, W. (and 13 others) 1997 Kinetics of response in lymphoid tissues to antiretroviral therapy of HIV-1 infection. *Science* **276**, 960–964. (Erratum in *Science* **276**, 1321.)
- Chun, T. W. (and 14 others) 1997 Quantification of latent tissue reservoirs and total body viral load in HIV-1 infection. *Nature* **387**, 183–188.
- Deacon, N. J. (and 19 others) 1995 Genomic structure of an attenuated quasi species of HIV-1 from a blood transfusion donor and recipients. *Science* **270**, 988–991.
- De Boer, R. J. & Perelson, A. S. 1998 Target cell limited and immune control models of HIV infection: a comparison. *J. Theor. Biol.* **190**, 201–214.
- De Boer, R. J., Boucher, C. A. & Perelson, A. S. 1998 Target cell availability and the successful suppression of HIV by hydroxyurea and didanosine. *AIDS* **12**, 1567–1570.
- Embertson, J., Zupancic, M., Ribas, J. L., Burke, A., Racz, P., Tenner-Racz, K. & Haase, A. T. 1993 Massive covert infection of helper T lymphocytes and macrophages by HIV during the incubation period of AIDS. *Nature* **362**, 359–362.
- Fauci, A. S. 1993 Multifactorial nature of human immunodeficiency virus disease: implications for therapy. *Science* **262**, 1011–1018.
- Fleury, S. (and 19 others) 1998 Limited CD4⁺ T-cell renewal in early HIV-1 infection: effect of highly active antiretroviral therapy. *Nature Med.* **4**, 794–801.
- Ginzburg, L. R. & Akçakaya, H. R. 1992 Consequences of ratio-dependent predation for steady-state properties of ecosystems. *Ecology* **93**, 1536–1543.
- Goulder, P. J. (and 11 others) 1997 Late escape from an immunodominant cytotoxic T-lymphocyte response associated with progression to AIDS. *Nature Med.* **3**, 212–217.
- Haase, A. T. (and 13 others) 1996 Quantitative image analysis of HIV-1 infection in lymphoid tissue. *Science* **274**, 985–989.
- Hellerstein, M. (and 11 others) 1999 Directly measured kinetics of circulating T lymphocytes in normal and HIV-1-infected humans. *Nature Med.* **5**, 83–89.
- Ho, D. D., Newmann, A. U., Perelson, A. S., Chen, W., Leonard, J. M. & Markowitz, M. 1995 Rapid turnover of plasma virions and CD4 lymphocytes in HIV-1 infection. *Nature* **373**, 123–126.

- Hockett, R. D., Michael Kilby, J., Derdeyn, C. A., Saag, M. S., Sillers, M., Squires, K., Chiz, S., Nowak, M. A., Shaw, G. M. & Bucy, R. P. 1999 Constant mean viral copy number per infected cell in tissues regardless of high, low, or undetectable plasma HIV RNA. *J. Exp. Med.* **189**, 1545–1554.
- Jin, X. (and 13 others) 1999 Dramatic rise in plasma viremia after CD8(+) T cell depletion in simian immunodeficiency virus-infected macaques. *J. Exp. Med.* **189**, 991–998.
- Katzenstein, T. L., Pedersen, C., Nielsen, C., Lundgren, J. D., Jakobsen, P. H. & Gerstoft, J. 1996 Longitudinal serum HIV RNA quantification: correlation to viral phenotype at sero-conversion and clinical outcome. *AIDS* **10**, 167–173.
- Kaunzinger, C. M. K. & Morin, P. J. 1998 Productivity controls food-chain properties in microbial communities. *Nature* **395**, 495–497.
- Klennerman, P., Phillips, R. E., Rinaldo, C. R., Wahl, L. M., Ogg, G., May, R. M., McMichael, A. J. & Nowak, M. A. 1996 Cytotoxic T lymphocytes and viral turnover in HIV type 1 infection. *Proc. Natl Acad. Sci. USA* **93**, 15 323–15 328.
- McLean, A. R. & Nowak, M. A. 1992 Competition between zidovudine-sensitive and zidovudine-resistant strains of HIV. *AIDS* **6**, 71–79.
- McLean, A. R., Emergy, V. C., Webster, A. & Griffiths, P. D. 1991 Population dynamics of HIV within an individual after treatment with zidovudine. *AIDS* **5**, 485–489.
- Mellors, J. W., Rinaldo Jr, C. R., Gupta, P., White, R. M., Todd, J. A. & Kingsley, L. A. 1996 Prognosis in HIV-1 infection predicted by the quantity of virus in plasma. *Science* **272**, 1167–1170. [Erratum in *Science* **275**, 14.]
- Mittler, J. E., Markowitz, M., Ho, D. D. & Perelson, A. S. 1999 Improved estimates for HIV-1 clearance rate and intracellular delay. *AIDS* **13**, 1415–1417.
- Mori, K. (and 10 others) 2000 Suppression of acute viremia by short-term postexposure prophylaxis of simian/human immunodeficiency virus SHIV-RT-infected monkeys with a novel reverse transcriptase inhibitor (GW420867) allows for development of potent antiviral immune response resulting in efficient containment of infection. *J. Virol.* **74**, 5747–5753.
- Notermans, D. W., Goudsmit, J., Danner, S. A., De Wolf, F., Perelson, A. S. & Mittler, J. 1998 Rate of HIV-1 decline following antiretroviral therapy is related to viral load at baseline and drug regimen. *AIDS* **12**, 1483–1490.
- Nowak, M. A. & Bangham, C. R. 1996 Population dynamics of immune responses to persistent viruses. *Science* **272**, 74–79.
- Ogg, G. S. (and 14 others) 1998 Quantitation of HIV-1-specific cytotoxic T lymphocytes and plasma load of viral RNA. *Science* **279**, 2103–2106.
- Ogg, G. S. (and 13 others) 1999 Decay kinetics of human immunodeficiency virus-specific effector cytotoxic T lymphocytes after combination antiretroviral therapy. *J. Virol.* **73**, 797–800.
- Orendi, J. M., Bloem, A. C., Borleffs, J. C., Wijnholds, F. J., De Vos, N. M., Nottet, H. S., Visser, M. R., Snippe, H., Verhoef, J. & Boucher, C. A. 1998 Activation and cell cycle antigens in CD4+ and CD8+ T cells correlate with plasma human immunodeficiency virus (HIV-1) RNA level in HIV-1 infection. *J. Infect. Dis.* **178**, 1279–1287.
- Oxenius, A., Price, D. A., Easterbrook, P. J., O'Callaghan, C. A., Kelleher, A. D., Whelan, J. A., Sontag, G., Sewell, A. K. & Phillips, R. E. 2000 Early highly active antiretroviral therapy for acute HIV-1 infection preserves immune function of CD8+ and CD4+ T lymphocytes. *Proc. Natl Acad. Sci. USA* **97**, 3382–3387.
- Pantaleo, G., Graziosi, C., Demarest, J. F., Butini, L., Montroni, M., Fox, C. H., Orenstein, J. M., Kotler, D. P. & Fauci, A. S. 1993 HIV infection is active and progressive in lymphoid tissue during the clinically latent stage of disease. *Nature* **362**, 355–358.
- Perelson, A. S., Neumann, A. U., Markowitz, M., Leonard, J. M. & Ho, D. D. 1996 HIV-1 dynamics *in vivo*: virion clearance rate, infected cell life-span, and viral generation time. *Science* **271**, 1582–1586.
- Piatk Jr, M., Saag, M. S., Yang, L. C., Clark, S. J., Kappes, J. C., Luk, K. C., Hahn, B. H., Shaw, G. M. & Lifson, J. D. 1993 High levels of HIV-1 in plasma during all stages of infection determined by competitive PCR. *Science* **259**, 1749–1754.
- Ramratnam, B., Bonhoeffer, S., Binley, J., Hurley, A., Zhang, L., Mittler, J. E., Markowitz, M., Moore, J. P., Perelson, A. S. & Ho, D. D. 1999 Rapid production and clearance of HIV-1 and hepatitis C virus assessed by large volume plasma apheresis. *Lancet* **354**, 1782–1785.
- Rinaldo, C. (and 10 others) 1995 High levels of anti-human immunodeficiency virus type 1 (HIV-1) memory cytotoxic T-lymphocyte activity and low viral load are associated with lack of disease in HIV-1-infected long-term nonprogressors. *J. Virol.* **69**, 5838–5842.
- Rosenzweig, M. L. 1971 Paradox of enrichment: destabilization of exploitation ecosystems in ecological time. *Science* **171**, 385–387.
- Schmitz, J. E. (and 15 others) 1999 Control of viremia in simian immunodeficiency virus infection by CD8+ lymphocytes. *Science* **283**, 857–860.
- Stilianakis, N. I., Boucher, C. A., De Jong, M. D., Van Leeuwen, R., Schuurman, R. & De Boer, R. J. 1997 Clinical data sets of human immunodeficiency virus type 1 reverse transcriptase-resistant mutants explained by a mathematical model. *J. Virol.* **71**, 161–168.
- Wei, X. (and 11 others) 1995 Viral dynamics in human immunodeficiency virus type 1 infection. *Nature* **373**, 117–122.
- Weiss, R. A. 1993 How does HIV cause AIDS? *Science* **260**, 1273–1279.
- Zhang, Z. Q. (and 16 others) 1998 Kinetics of CD4+ T cell repopulation of lymphoid tissues after treatment of HIV-1 infection. *Proc. Natl Acad. Sci. USA* **95**, 1154–1159.

As this paper exceeds the maximum length normally permitted, the authors have agreed to contribute to production costs.